Models for Deep Hydrodesulfurization of Alkylated Benzothiophenes. Reductive Cleavage of C−S Bonds Mediated by Precoordination of Manganese Tricarbonyl to the Carbocyclic Ring

Huazhi Li, Kunquan Yu, Eric J. Watson, Kurtis L. Virkaitis, Jason S. D'Acchioli, Gene B. Carpenter, and D. A. Sweigart*

Department of Chemistry, Brown University, Providence, Rhode Island 02912

Paul T. Czech, Kenneth R. Overly, and Fred Coughlin

Department of Chemistry, Providence College, Providence, Rhode Island 02918

Received October 11, 2001

The reduction of (η^6-benzothiophene)Mn(CO)$_3^+$ with cobaltocene under CO leads to insertion of the Mn(CO)$_4^-$ fragment into the C(aryl)−S bond to afford a neutral bimetallic complex. When there are methyl substituents at the 2,3-, 2,7-, or 3,7-positions, the regioselectivity and product distribution in the reductive insertion reactions are significantly affected, and several new types of complexes are formed. Low-temperature chemical reduction of (η^6-benzothiophene)Mn(CO)$_3^+$ complexes affords unstable η^4-species, (η^4-BT)Mn(CO)$_3^-$, which do not react with the η^6-cation to give insertion products. Similarly, electrochemical reduction of (η^6-benzothiophene)Mn(CO)$_3^+$ changes from a one-electron chemically irreversible process at room temperature to a two-electron chemically reversible but electrochemically irreversible process at −90 °C. It is concluded from these results that the room-temperature reductive cleavage of a C−S bond in (η^6-benzothiophene)Mn(CO)$_3^+$ occurs by a radical mechanism. Crystallographic data and density function theory (DFT) calculations indicate that insertion into the C(aryl)−S and not the C(vinyl)−S bond of (η^6-benzothiophene)Mn(CO)$_3^+$ is favored. A redetermination of the crystal structure of the η^1-S complex (η^1-3-MeBT)Re(Cp*)(CO)$_2$ revealed that the C(aryl)−S and C(vinyl)−S bonds are of similar lengths, suggesting that an η^1-S intermediate is not predisposed to insert into the latter bond, as was previously thought. DFT calculations of (η^6-BT)Mn(CO)$_3^+$ bonded in an η^1-S fashion to Mn(CO)$_4^-$ indicated that an intermediate of this sort is viable in the C−S insertion reactions.

Introduction

The hydrodesulfurization (HDS) of petroleum feedstocks is a heterogeneously catalyzed reaction that is necessary for both industrial and environmental reasons.[1] While the sulfur in petroleum can be found in a variety of species, compounds containing the resonance-stabilized thiophene ring are of special interest because they are the most difficult to treat with current hydroprocessing methodologies. This is particularly true of benzothiophenes (BT) and dibenzothiophenes (DBT) with alkyl substituents adjacent to the sulfur atom.[1,2] For this reason, the successful processing of such thiophenic materials is termed "deep hydrodesulfurization".

A variety of organometallic systems have been studied as models for the homogeneous HDS of thiophenes.[3] In particular, a substantial amount of research has been directed at C−S bond cleavage reactions of benzothiophenes. Most studies have utilized highly reactive coordinatively unsaturated nucleophilic metal fragments, which generally insert into the C(vinyl)−S bond in **1** to afford the metallathiacycle **2**. Insertion into the stronger C(aryl)−S bond in *free* unsubstituted benzothiophene to afford **3** has not been observed, although Cp*Rh(PMe$_3$) reacts with 2-MeBT to give **2** as the kinetic product, which then undergoes an intramolecular isomerization to a mixture of **2** and **3**.[4]

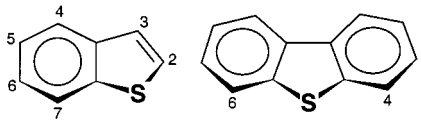

BT DBT

(1) Topsøe, H.; Clausen, B. A.; Massoth, F. E. *Hydrotreating Catalysis*; Springer: Berlin, 1996. (b) *Petroleum Chemistry and Refining*; Speight, J. G., Ed.; Taylor & Francis: Washington, DC, 1998.

(2) Shih, S. S.; Mizahi, S.; Green, L. A.; Sarli, M. S. *Ind. Eng. Chem. Res.* **1992**, *31*, 1232. (b) Topsøe, H.; Gates, B. C. *Polyhedron* **1997**, *16*, 3212.

(3) Sanchez-Delgado, R. A. *J. Mol. Catal.* **1994**, *86*, 287. (b) Angelici, R. J. *Polyhedron* **1997**, *16*, 3073. (c) Angelici, R. J. *Organometallics* **2001**, *20*, 1259. (d) Bianchini, C.; Meli. *J. Chem. Soc., Dalton Trans.* **1996**, 801. (e) Bianchini, C.; Meli, A. *Acc. Chem. Res.* **1998**, 31, 109. (f) Rauchfuss, T. B. *Prog. Inorg. Chem.* **1991**, *39*, 259. (g) Vicic, D. A.; Jones, W. D. *J. Am. Chem. Soc.* **1999**, *121*, 7606. (h) Garcia, J. J.; Mann, B. E.; Adams, H.; Bailey, N. A.; Maitlis, P. M. *J. Am. Chem. Soc.* **1995**, *117*, 2179.

(4) Myers, A. W.; Jones, W. D.; McClements, S. M. *J. Am. Chem. Soc.* **1995**, *117*, 11704.

10.1021/om0108907 CCC: $22.00
Publication on Web 02/16/2002

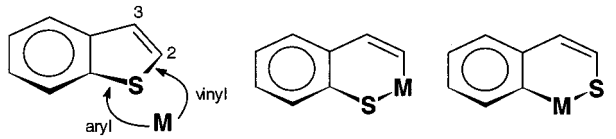

1 **2** **3**

An alternative to the use of highly reactive transition metal fragments to cleave C−S bonds in benzothiophenes is to induce the requisite activation by precoordination of a metal to the carbocyclic ring. Thus, coordination of the electrophilic fragment $Mn(CO)_3^+$ results in "remote activation" of the thiophene ring in **4** to facile C−S bond cleavage by mild nucleophiles, e.g., $Pt(PPh_3)_2$, to generate the metallathiacycle **5** shown in eq 1.[5] It has also been shown that **4** is very susceptible to *reductive cleavage* of a C−S bond according to eq 2.[6] That the C(aryl)−S bond, rather than the weaker C(vinyl)−S bond, is cleaved in eq 2 is a unique feature of this reaction. When the benzothiophene complex possesses a methyl or ethyl substituent at the 7-position, the C(aryl)−Mn−S insertion product **6** is rapidly formed, but is followed by a spontaneous room-temperature isomerization to the C(vinyl)−Mn−S product **7**, as shown in eq 3.[6b]

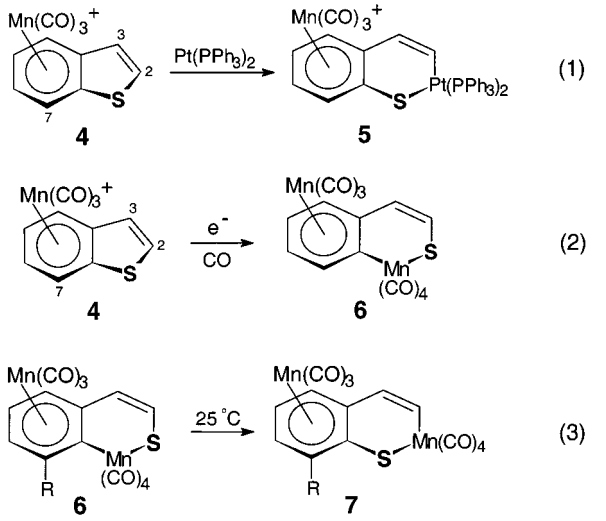

In the present study, the effect of methyl substitution at the benzothiophene 2-, 3-, and/or 7-positions on the reductive cleavage of the C−S bonds is examined. The mechanism of manganese insertion into the C−S bonds was probed by synthetic, low-temperature IR, and electrochemical techniques. In concert with this, X-ray structural determinations and theoretical calculations were utilized to study the factors determining the regioselectivity of the C−S cleavage reactions. Finally, experiments are reported that provide mechanistic insight into the migration reaction typified by eq 3. In view of the marked influence of alkyl substitutents in determining the HDS reactivity of BTs and DBTs, it is felt that the results presented herein may shed light on the possible reaction pathways available on a catalyst surface.

Results and Discussion

Product Distributions for Manganese Insertion into C−S Bonds. The effect of methyl substitution on reductive C−S bond cleavage was studied with the manganese tricarbonyl complexes of 2,3-, 2,7-, and 3,7-Me_2BT. The product distributions are indicated in Scheme 1. In all cases, the reactions were performed at room temperature with cobaltocene reductant under an atmosphere of CO.

Since the unsubstituted benzothiophene complex **4** was known to give C(aryl)−S bond scission upon reduction (eq 2), it was anticipated that the 2,3-Me_2BT complex **8** would similarly undergo C(aryl)−S bond insertion. Indeed, cobaltocene reduction of **8** was found to afford **9** in 60% yield (based on available manganese), along with traces of two additional products identified as **10** and **11**. The yield of complex **10**, in which the sulfur in the metallathiacyclic ring functions as a ligand to a $Mn_2(CO)_8$ moiety, increased to 69% when $Mn_2(CO)_{10}$ was added to the reaction mixture. Sulfur binding to $Mn_2(CO)_8$ as seen in **10** had previously been observed[6d] to result from reductive insertion with (η^6-dibenzothiophene)$Mn(CO)_3^+$. The existence and stability of species such as **10** demonstrates the greatly enhanced nucleophilicity of the sulfur atom that results from metal insertion into a C−S bond in benzothiophene.[6a] The crystal structure of **10** is shown in Figure 1. Selected bond lengths and angles, given in the legend, are quite similar to those found for the dibenzothiophene analogue.[6d]

Complex **11**, obtained in only trace amounts, was characterized by X-ray diffraction (Figure 2). It features C(aryl)−S insertion into two benzothiophene molecules, which are then coupled via Mn−Mn and Mn−S bonds. Hydrogenolysis (protonation) of one of the Mn−S bonds has also occurred to give a free phenyl substituent that has lost its η^6-coordinated $Mn(CO)_3^+$ moiety.

The reaction of the 2,7-Me_2BT complex **12** with cobaltocene gave a relatively low combined 34% yield of three products, each of which was isolated and characterized (Scheme 1). Insertion of $Mn(CO)_4$ into both C(aryl)−S and C(vinyl)−S bonds occurred to afford **13** (13% yield) and **14** (10% yield), respectively. Significantly, neither **13** nor **14** was found to interconvert in solution (CH_2Cl_2, 24 h), demonstrating that neither is an intermediate in the formation of the other. The methyl substituents in **12** provide a measure of steric hindrance to insertion into either C−S bond, and this may account for the rather low yield of the isomeric **13** and **14**. A third product obtained from the reduction reaction, complex **15** (11% yield), was found to have the crystal structure shown in Figure 3. Complex **15** is thermally stable, with no change found after 24 h in refluxing CH_2Cl_2, and is structurally related to a rhenium complex recently prepared from the reaction of

(5) Yu, K.; Li, H.; Watson, E. J.; Virkaitis, K. L.; Carpenter, G. B.; Sweigart, D. A. *Organometallics* **2001**, *20*, 3550. (b) Dullaghan, C. A.; Zhang, X.; Greene, D. L.; Carpenter, G. B.; Sweigart, D. A.; Camiletti, C.; Rajaseelan, E. *Organometallics* **1998**, *17*, 3316. (c) Li, H.; Carpenter, G. B.; Sweigart, D. A. *Organometallics* **2000**, *19*, 1823.

(6) Dullaghan, C. A.; Sun, S.; Carpenter, G. B.; Weldon, B.; Sweigart, D. A. *Angew. Chem., Int. Ed.* **1996**, *35*, 212. (b) Dullaghan, C. A.; Zhang, X.; Walther, D.; Carpenter, G. B.; Sweigart, D. A.; Meng, Q. *Organometallics* **1997**, *16*, 5604. (c) Dullaghan, C. A.; Carpenter, G. B.; Sweigart, D. A.; Choi, D. S.; Lee, S. S.; Chung, Y. K. *Organometallics* **1997**, *16*, 5688. (d) Zhang, X.; Dullaghan, C. A.; Carpenter, G. B.; Sweigart, D. A.; Meng, Q. *Chem. Commun.* **1998**, 93. (e) Zhang, X.; Dullaghan, C. A.; Watson, E. J.; Carpenter, G. B.; Sweigart, D. A. *Organometallics* **1998**, *17*, 2067. (f) Zhang, X.; Watson, E. J.; Dullaghan, C. A.; Gorun, S. M.; Sweigart, D. A. *Angew. Chem., Int. Ed.* **1999**, *38*, 2206.

Scheme 1

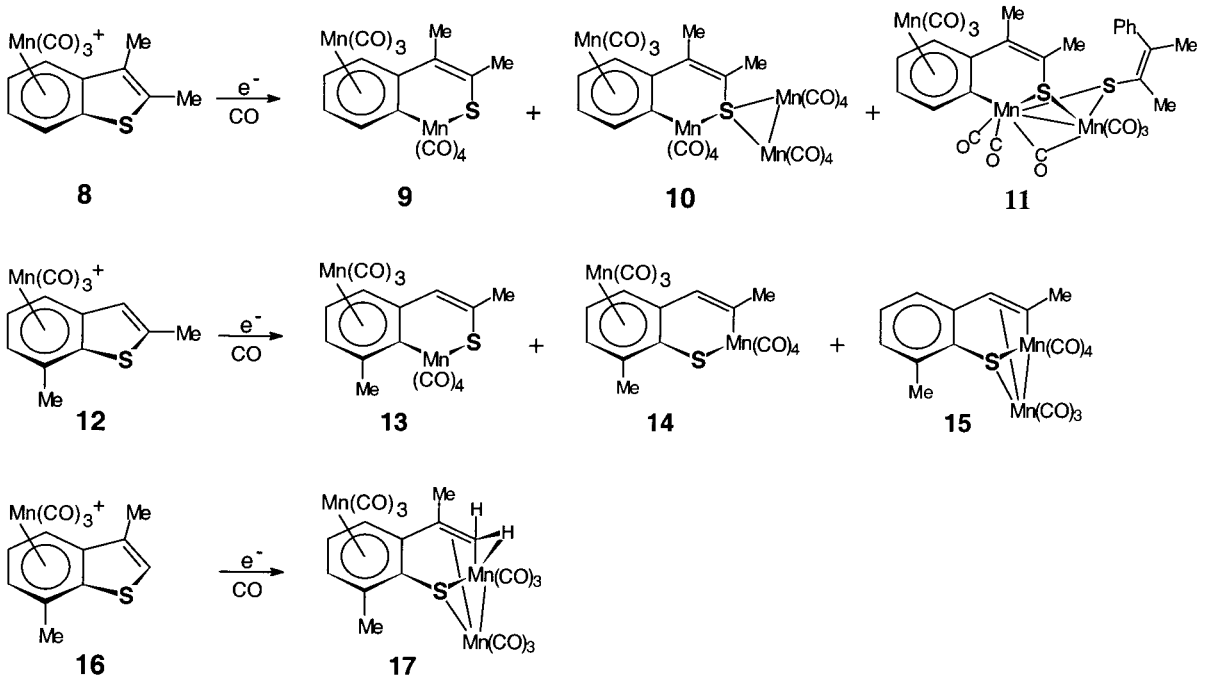

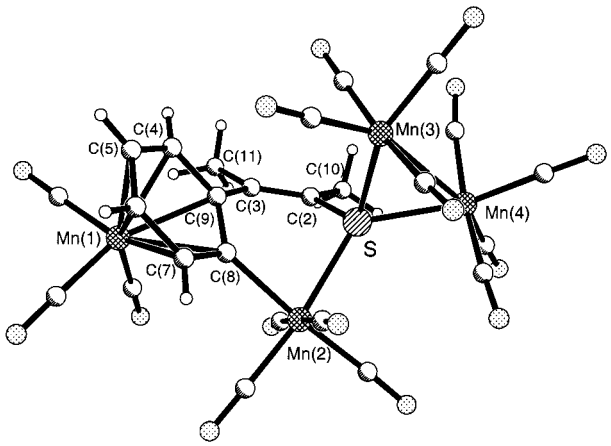

Figure 1. Crystal structure of **10**. Selected bond lengths (Å) and angles (deg): C(8)−Mn(2) 2.087(2), S−Mn(2) 2.3968(7), S−C(2) 1.808(2), C(2)−C(3) 1.328(4), C(3)−C(9) 1.487(3), S−Mn(3) 2.3174(7), S−Mn(4) 2.3072(7), Mn(3)−Mn(4) 2.7682(6), C(8)−S−C(2) 80.75(7), Mn(2)−S−C(2) 97.66(8).

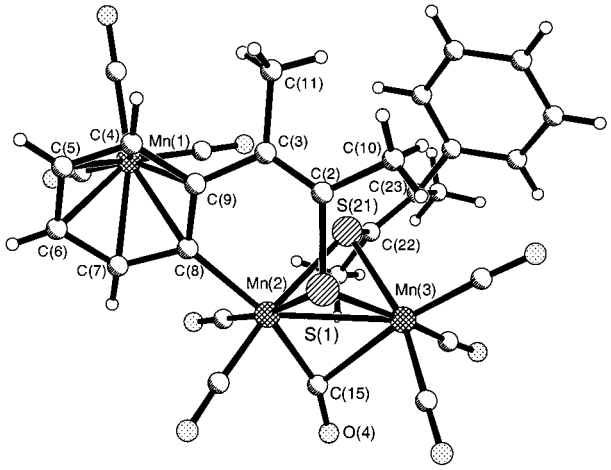

Figure 2. Crystal structure of **11**. Selected bond lengths (Å) and angles (deg): C(8)−Mn(2) 2.078(5), S(1)−Mn(2) 2.3118(15), S(1)−Mn(3) 2.3199(16), S(1)−C(2) 1.771(5), C(2)−C(3) 1.341(7), C(3)−C(9) 1.479(7), S(21)−Mn(2) 2.3933(15), S(21)−Mn(3) 2.3162(16), Mn(2)−Mn(3) 2.6578-(11), C(22)−S(21) 1.787(6), C(22)−C(23) 1.340(8), C(8)−Mn(2)−S(1) 86.66(14), Mn(2)−S(1)−C(2) 106.60(18).

free benzothiophene and $Re_2(CO)_{10}$ under photolytic conditions.[7]

As shown in Scheme 1, reduction of the 3,7-Me_2BT complex **16** led to a 55% isolated yield of the very interesting trimetallic **17**, the structure of which was verified by X-ray diffraction. As illustrated in Figure 4, insertion into the C(vinyl)−S bond of **16** occurred to afford a structure that is in some ways analogous to that seen in **15**, but with several very significant differences. Complex **17** retains the $Mn(CO)_3^+$ moiety bonded to the carbocyclic ring, and the inserted manganese atom labeled Mn(2) in Figures 3 and 4 contains four CO ligands in **15**, but three in **17**. Most significantly, in **17** there is a new C−H bond, labeled C(2)−H(2b), that is agostically bonded to Mn(2). The "extra" hydrogen atom may have originated from the solvent or from the alumina used during chromatographic workup. During X-ray data refinement, all 11 atoms in structure **17** appeared clearly in a difference map. To best define the agostic bonding, each hydrogen was refined independently with isotropic displacement parameters. All 11 hydrogens refined to physically reasonable positions, with the Mn(2)−H(2b) agostic bond length being 1.82(3) Å, which is a value similar to ones reported in the literature for other manganese systems.[8] The agostic hydrogen H(2b) showed up clearly in the ^{1}H NMR at −11.5 ppm in CD_2Cl_2. This strong agostic C−H → Mn

(7) Reynolds, M. A.; Guzei, I. A.; Angelici, R. J. *Chem. Commun.* **2000**, 513. (b) Reynolds, M. A.; Guzei, I. A.; Angelici, R. J. *Organometallics* **2001**, *20*, 1071.

(8) Brookhart, M.; Lamanna, W.; Humphrey, M. B. *J. Am. Chem. Soc.* **1982**, *104*, 2117.

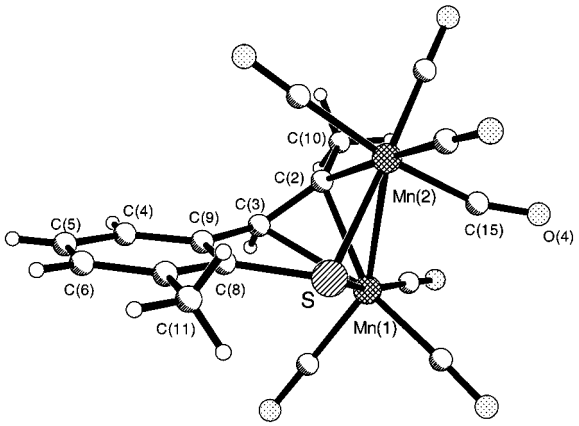

Figure 3. Crystal structure of **15**. Selected bond lengths (Å) and angles (deg): C(8)−S 1.779(2), S−Mn(1) 2.2937(6), S−Mn(2) 2.3757(6), Mn(2)−C(2) 2.073(2), C(2)−C(3) 1.390(3), C(3)−C(9) 1.487(3), Mn(1)−Mn(2) 2.6792(5), Mn(1)−C(2) 2.137(2), Mn(1)−C(3) 2.295(2), C(8)−S−Mn(2) 104.57(7), S−Mn(2)−C(2) 85.64(7).

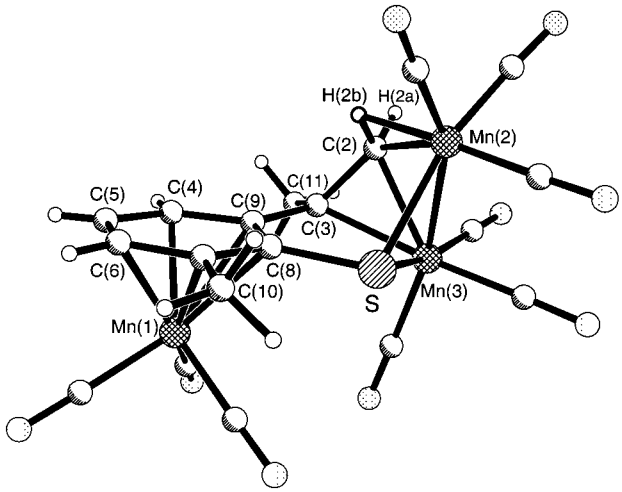

Figure 4. Crystal structure of **17**. Selected bond lengths (Å) and angles (deg): C(8)−S 1.763(3), S−Mn(2) 2.3257(8), S−Mn(3) 2.3086(9), Mn(2)−C(2) 2.145(3), C(2)−C(3) 1.460(4), Mn(2)−Mn(3) 2.6239(6), Mn(3)−C(2) 2.070(3), Mn(3)−C(3) 2.140(3), Mn(2)−H(2b) 1.82(3), C(8)−S−Mn(2) 104.94(9), S−Mn(2)−C(2) 82.68(8).

interaction is especially interesting because it can be seen as a possible first step in the hydrogenolysis of the Mn−C σ bond, which would be needed in any catalytic desulfurization process.

The synthetic results in Scheme 1 demonstrate that alkylation has a large effect on the regiochemistry and on the identity of the products that are formed. Steric interactions imposed by the methyl substituents are likely responsible for this diversity. A consideration of the product distributions seen is suggestive of a radical mechanism for the manganese insertion into the C−S bonds. To further probe the reaction mechanism of the C−S cleavage reactions, variable-temperature infrared and electrochemical experiments were performed on benzothiophene complexes not possessing substituents in the sterically sensitive 2- or 7-positions.

Infrared and Electrochemical Studies of the C−S Insertion Reactions. A mechanism for the reductive insertion of $Mn(CO)_4$ into the C(aryl)−S bond in (η^6-BT)$Mn(CO)_3^+$ (**4**) to afford the metallathiacycle **6** (eq 2) was previously proposed by us.[6e] The mechanistic details were predicated on the known[9] chemistry of (η^6-naphthalene)$Mn(CO)_3^+$, which readily undergoes ring slippage upon reduction to afford (η^4-naphthalene)$Mn(CO)_3^-$. The latter complex rapidly attacks the former to eliminate naphthalene and give characterized bimetallic species such as (η^6,η^4-naphthalene)$Mn_2(CO)_6$ (**18**).

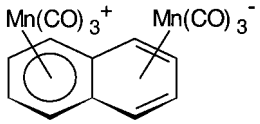

18

In analogy with this, the initial step in eq 2 was thought[6e] to be the two-electron reduction of half of the available (η^6-BT)$Mn(CO)_3^+$ to (η^4-BT)$Mn(CO)_3^-$. The latter η^4-slipped anionic complex then reacts rapidly with remaining cationic **4** to eliminate benzothiophene and produce a bimetallic species analogous to **18**, which undergoes subsequent insertion into a C−S bond. Unfortunately, however, the evidence presented below indicates that this mechanism is incorrect.

In situ variable-temperature infrared experiments in CH_2Cl_2 were performed to probe for intermediates in eq 2. For solubility and mechanistic reasons, the 5-MeBT and 3-MeBT complexes **19** and **20** were selected for study. At room temperature, both **19** and **20** under CO reacted cleanly and rapidly with cobaltocene to afford the C(aryl)−S insertion products analogous to **6**. In contrast, at −90 °C under CO, **19** was found to react rapidly with 1 equiv of cobaltocene to give a clean IR with ν_{CO} bands at 2005 and 1930 cm^{-1}. The position, intensity, and room-temperature persistence of these bands clearly indicate cyclohexadienyl species, probably formed as the result of ring coupling of neutral radicals (FAB MS data indicated a ring-coupled dimeric species). The important point here is that insertion into the C−S bond does not occur at −90 °C. Hence, the conclusion can be made that the (stable) product formed depends on the reaction temperature.

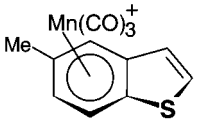

19

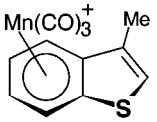

20

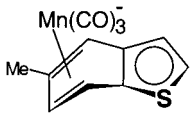

21

When 2 equiv of cobaltocene was added to **19** at −90 °C, clean formation of the η^4 anionic complex **21** was observed. Although this complex decomposed upon warming above −75 °C, it persisted for more than 30 min at −90 °C. On the basis of the spectral properties of the structurally characterized[10] stable complex (η^4-naphthalene)$Mn(CO)_3^-$, the low-temperature IR bands observed at 1933, 1839, and 1817 cm^{-1} for **21** are very diagnostic. The addition of 1 equiv of cation **19** to anion **21** at −90 °C led to rapid and clean formation of cyclohexadienyl complexes, with no C−S insertion found.

(9) Sun, S.; Dullaghan, C. A.; Carpenter, G. B.; Rieger, A. L.; Rieger, P. H.; Sweigart, D. A. *Angew. Chem., Int. Ed.* **1995**, *34*, 2540. (b) Sun, S.; Dullaghan, C. A.; Sweigart, D. A. *J. Chem. Soc., Dalton Trans.* **1996**, 4493.

(10) Thompson, R. L.; Lee, S.; Rheingold, A. L.; Cooper, N. J. *Organometallics* **1991**, *10*, 1657.

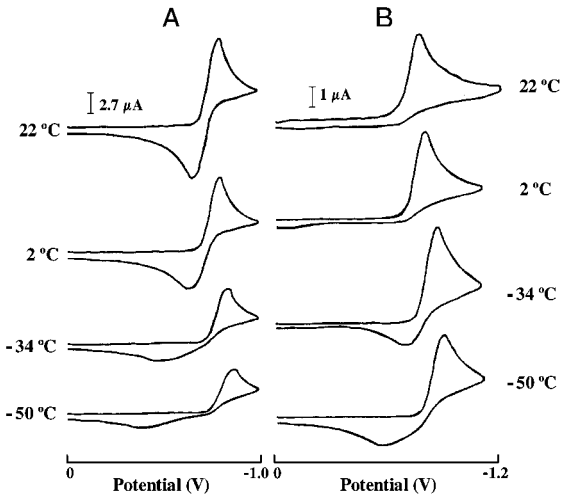

Figure 5. Cyclic voltammograms at the indicated temperature in CH_2Cl_2 with 0.10 M $[Bu_4N]PF_6$ electrolyte for (A) the naphthalene complex [**22**]BF_4 at 1.0 mM and (B) the benzothiophene complex [**19**]BF_4 at 1.0 mM. For all CVs the working electrode was a 1.0 mm diameter glassy carbon disk and the scan rate was 0.50 V/s. Potentials for A are relative to $E_{1/2}$(ferrocene) = 0.40 V and for B are relative to $E_{1/2}$(ferrocene) = 0.49 V.

This observation rules out the mechanism postulated earlier that C−S insertion comes about by reaction of the anion with the cation.

To test a possible mechanistic effect of a substituent on the thiophenic C=C double bond, complex **20** was studied at low temperatures. The results obtained at −90 °C were virtually the same as those seen with complex **19**. Thus, 1 equiv of cobaltocene gave rapid formation of cyclohexadienyl complexes (ν_{CO} = 2005, 1931 cm^{-1}). Two equivalents of cobaltocene produced the η^4-anion (ν_{CO} = 1935, 1841, 1818 cm^{-1}), which reacted rapidly with cation **20** to generate cyclohexadienyl complexes. As with **19**, no C−S insertion was found at −90 °C.

Electrochemical experiments performed with **19** complement the IR studies discussed above. Room-temperature bulk electrolysis of **19** under N_2 at a platinum working electrode consumed one electron and afforded the expected C−S insertion product along with lesser amounts of unidentified species. The cyclic voltammetric behavior of **19** in CH_2Cl_2 was recorded at variable temperatures and compared to that of the dimethoxynaphthalene complex **22**, which is known[9b,10,11] to undergo clean two-electron reduction to the anionic **23**. The results, illustrated in Figure 5, proved to be

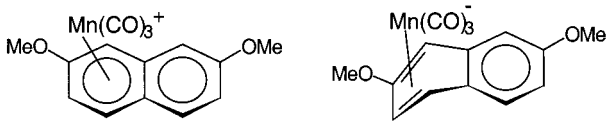

22 **23**

highly informative. As expected, the reduction of **22** was found to be chemically reversible at all temperatures. The large peak-to-peak separations at the lower temperatures are due to slow (irreversible) heterogeneous charge transfer that accompanies formation of the ring-slipped product **23**. In contrast, the benzothiophene complex **19** is reduced irreversibly by one electron at 22 °C. However, some chemical reversibility becomes evident at −34 °C and seems complete at −50 °C. A plot of the peak reduction current, i_p, versus temperature is given in Figure 6. It can be seen that for **22** i_p drops with temperature, as would be expected from the temperature dependence of the diffusion coefficient. With **19**, however, i_p is virtually independent of temperature. In conjunction with the IR results given above, one can confidently ascribe this unusual behavior to a change from an irreversible, one-electron reduction to a reversible, two-electron reduction as the temperature is lowered. In this way, the anticipated reduction in current due to a decreasing diffusion coefficient is roughly compensated by an increase in the effective number of electrons, with the result that the current is unchanged.

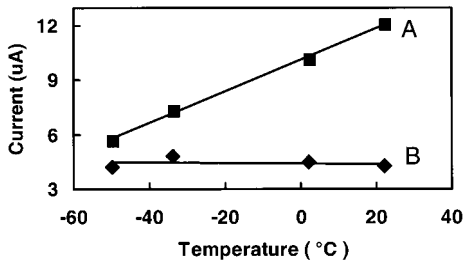

Figure 6. Plot of the peak reduction current i_p versus temperature for the CVs shown in Figure 5. Line A refers to [**22**]BF_4, and line B refers to [**19**]BF_4.

The infrared and electrochemical data, along with the synthetic results shown in Scheme 1, collectively indicate that the mechanism of reductive insertion into a C−S bond in coordinated benzothiophene is radical in nature. Although possible, it is unlikely that insertion at room temperature stems from an (η^4-benzothiophene)-$Mn(CO)_3^-$ anion reacting with an (η^6-benzothiophene)-$Mn(CO)_3^+$ cation, since these species were shown to react at low temperature by ring-coupling and not C−S scission.

Structural and Theoretical Aspects of the C−S Insertion Reactions. It was pointed out in the Introduction that metal nucleophiles generally insert into the C(vinyl)−S bond of benzothiophenes. Insertion of $Mn(CO)_4$ into benzothiophenes containing the $Mn(CO)_3^+$ moiety precoordinated to the carbocyclic ring is an exception to this rule, as illustrated by eq 2. Indeed, the fact that sterically driven isomerization of C(aryl)−Mn−S to C(vinyl)−Mn−S metallathiacycles is possible (eq 3) demonstrates that precoordination of a metal to the carbocyclic ring in BTs results in regioselective activation favoring C(aryl)−S over C(vinyl)−S scission, even when the latter is the thermodynamic product.

In a theoretical study, Harris examined the factors that determine whether it is the C(aryl)−S or the C(vinyl)−S bond in BT that is cleaved upon metal insertion.[12] It has been suggested numerous times[3,13,14] that C−S insertion is preceded by η^1-S coordination to the entering metal fragment. In agreement with the generally observed C(vinyl)−S insertion, an X-ray

(11) Virkiatis, K. L.; Sun, S.; Sweigart, D. A. Unpublished results.

(12) Palmer, M. S.; Rowe, S.; Harris, S. *Organometallics* **1998**, *17*, 3798.

(13) Choi, M.-G.; Angelici, R. J. *Organometallics* **1992**, *11*, 3328.

Table 1. Crystallographic Data for 10, 11, 15, 17, and 24

	10	11	15	17	24
formula	$C_{25}H_{10}Mn_4O_{15}S$	$C_{29}H_{21}Mn_3O_9S_2$	$C_{17}H_{10}Mn_2O_7S$	$C_{19}H_{11}Mn_3O_9S$	$C_{21}H_{23}O_2ReS$
fw	802.15	742.40	468.19	580.16	525.65
temperature	298	298	298	298	298
wavelength	0.71073	0.71073	0.71073	0.71073	0.71073
cryst syst	triclinic	monoclinic	orthorhombic	orthorhombic	monoclinic
space group	$P\bar{1}$	$P2_1/c$	$P2_12_12_1$	$Pbca$	$P2_1/n$
a, Å	10.0455(9)	12.3253(13)	7.7296(2)	15.3845(18)	8.6970(11)
b, Å	10.2361(9)	28.058(3)	10.1572(4)	14.0113(13)	13.6950(17)
c, Å	15.1945(14)	9.4885(10)	23.5412(9)	19.7753(14)	16.583(2)
α, deg	96.964(2)	90	90	90	90
β, deg	95.061(2)	111.599(2)	90	90	91.350(3)
γ, deg	102.288(2)	90	90	90	90
V, Å^3	1504.8(2)	3050.9(5)	1848.25(11)	4262.7(7)	1974.5(4)
Z	2	4	4	8	4
d_{calcd}, g cm^{-3}	1.770	1.616	1.683	1.808	1.768
μ, mm^{-1}	1.780	1.411	1.515	1.897	6.270
F(000)	792	1496	936	2304	1024
cryst dimens, mm	0.29 × 0.26 × 0.20	0.13 × 0.13 × 0.09	0.30 × 0.20 × 0.19	0.25 × 0.16 × 0.12	0.49 × 0.48 × 0.41
θ range, deg	1.36−28.37	1.78−26.37	1.73−28.26	2.06−26.37	1.93−28.32
no. of reflns collecd	24 173	44 548	29 492	58 637	13 869
no. of indept reflns	7227 (R_{int} = 0.0786)	6234 (R_{int} = 0.1276)	4548 (R_{int} = 0.0654)	4354 (R_{int} = 0.1040)	4602 (R_{int} = 0.0285)
no. of data/restraints/params	7227/0/408	6234/0/392	4548/0/246	4354/0/333	4602/27/294
GOF on F^2	1.054	1.008	1.047	1.120	1.171
R1, wR2 [$I > 2\sigma(I)$]	0.0417, 0.0993	0.0565, 0.1178	0.0279, 0.0674	0.0324, 0.0730	0.0295, 0.0667
R1, wR2 (all data)	0.0580, 0.1093	0.1350, 0.1487	0.0329, 0.0703	0.0505, 0.0868	0.0369, 0.0688

crystal structure of the η^1-S complex **24** revealed a

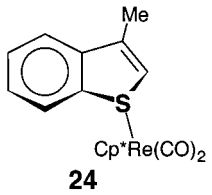

24

C(vinyl)−S bond elongated by ca. 0.2 Å in comparison to the C(aryl)−S bond.[13] This, of course, nicely accounts for subsequent selective insertion into the C(vinyl)−S bond. However, calculations by Harris did not predict the reported differential elongation of the C(vinyl)−S bond in **24**, and it was suggested that additional η^1-S structures are needed to establish whether such coordination selectively activates the C(vinyl)−S bond.[12] With respect to manganese insertion reactions such as eq 2, which result in C(aryl)−S cleavage, the assertion that η^1-S bonding leads to C(vinyl)−S cleavage is especially relevant since it would mean that an η^1-S−$Mn(CO)_4$ intermediate must be excluded from consideration in these reactions.

Following Harris' observation that the reported structure of **24** contained anomalies that cast doubt on the validity of the refined C(vinyl)−S bond length, we decided to redetermine the structure. The result is shown in Figure 7, and crystal data are given in Table 1. The structure proved to be very similar to that reported by Choi and Angelici,[13] except for a degree of disorder observed in the 3-MeBT ligand. Reexamination of the earlier data, kindly provided by Professor Angelici, showed that similar disorder was present in that case also. The disorder in the 3-MeBT group, which was more apparent in our work because of a larger crystal and more extensive data set, was very successfully modeled as a major configuration (62% occupancy) along with a minor component that is a mirror image of the former and lies in the same plane. The sulfur atoms of the major and minor components are separated by 0.67 Å. The chief consequence of modeling the disorder is that the two C−S bonds now have very similar lengths: C(aryl)−S 1.737(7), C(vinyl)−S 1.746(14) Å. Without recognition of the disorder, the sulfur position is shifted away from that of the major component toward the minor component, thereby lengthening the *apparent* distance to C(vinyl) and shortening the *apparent* distance to C(aryl). However, the conclusion from our results that the C(vinyl)−S and C(aryl)−S bonds are about the same length suggests that neither is differentially activated in **24**. Consequently, η^1-S species remain viable intermediates for insertion into either bond.

In the particular case of $Mn(CO)_4$ insertion, a density functional theory (DFT) calculation of the η^1-S species **25** was performed. The resulting structure is illustrated

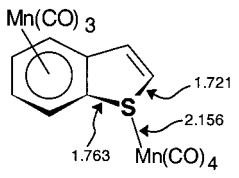

25

in Figure 8. The interesting and unusual feature of the calculation is the nearly in-plane position of the Mn atom, which contrasts with structures of η^1-S complexes determined by X-ray diffraction.[13,15] The latter invariably have the metal−sulfur bond vector 40−60° out of the thiophenic plane, so that the sulfur is best described

(14) Dong, L.; Duckett, S. B.; Ohman, K. F.; Jones, W. D. *J. Am. Chem. Soc.* **1992**, *114*, 151. (b) Bianchini, C.; Herrera, V.; Jimenez, M. V.; Meli, A.; Sánchez-Delgado, R. A.; Vizza, F. *J. Am. Chem. Soc.* **1995**, *117*, 8567. (c) Mills, P.; Korlann, S.; Bussell, M. E.; Reynolds, M. A.; Ovchinnikov, M. V.; Angelici, R. J.; Stinner, C.; Weber, T.; Prins, R. *J. Phys. Chem. A* **2001**, *105*, 4418.

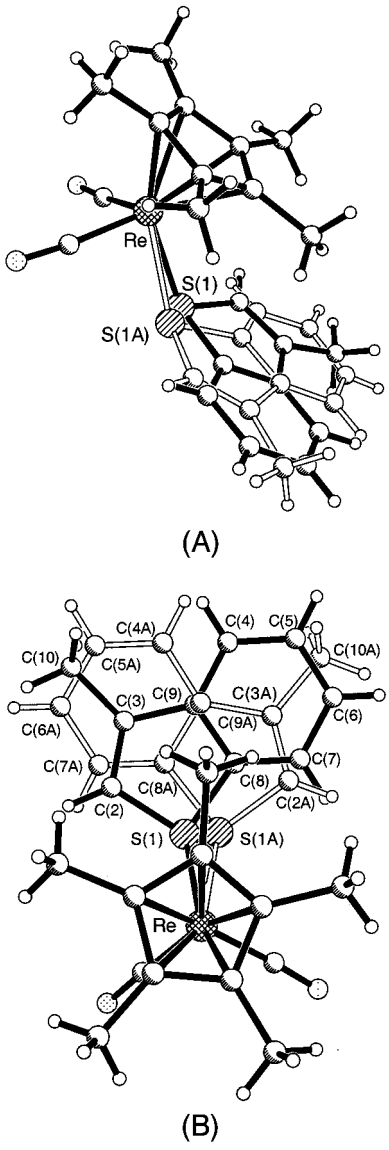

Figure 7. Two views of the crystal structure of **24**, showing the disordered 3-MeBT ligands. The major component (62%) is shown with darkened bonds and the minor component (38%) with open bonds. The disordered 3-MeBT ligands are mirror images of each other and are coplanar. Selected bond lengths (Å) and angles (deg) in the major configuration: Re−S 2.349(2), Re−C(21) 1.8697(15), Re−C(22) 1.8796(16), S−C(2) 1.746(14), S−C(8) 1.737(7), C(2)−C(3) 1.343(15), C(3)−C(9) 1.45(2), C(3)−C(10) 1.512(14), C(8)−C(9) 1.408(12), C(2)−S−C(8) 92.0(6), S−C(2)−C(3) 111.5(10), C(2)−C(3)−C(9) 113.9(8), C(3)−C(9)−C(8) 111.2(9), S−C(8)−C(9) 110.7(9), Re−S−C(2) 117.7(5), Re−S−C(8) 117.3(3).

as "sp^3" hybridized. With **25** the calculated angle is only 4°. Probably related to this unusual position is a calculated Mn−S bond length (2.156 Å) that is extremely short, suggesting significant metal−sulfur π-interaction. The C(aryl)−S bond is calculated to be somewhat longer than the C(vinyl)−S bond, but probably not enough to constitute substantial evidence that

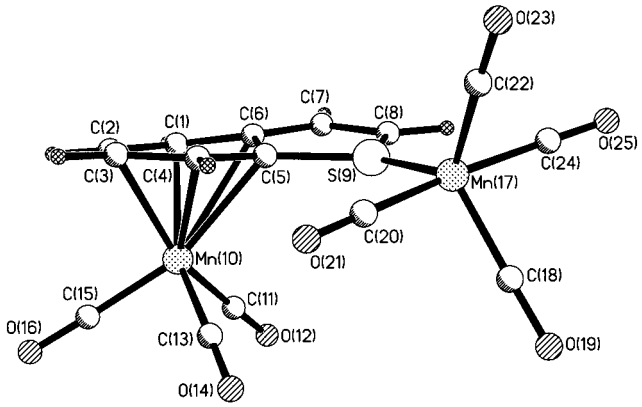

Figure 8. Structure of the η^1-S complex **25** as calculated by density functional theory at the B3LYP/DZVP level. Selected calculated bond lengths (Å): Mn(17)−S(9) 2.156, S(9)−C(5) 1.763, S(9)−C(8) 1.721, C(8)−C(7) 1.395, C(7)−C(6) 1.395, C(5)−C(6) 1.463, Mn(17)−C(18) 1.817, C(18)−O(19) 1.163, Mn(10)−C(15) 1.815, C(15)−O(16) 1.157.

25 is, in fact, an intermediate in the observed insertion of $Mn(CO)_4$ into the former bond.

With respect to the regioselectivity of insertion, Harris calculated[12] that precoordination of a metal to the carbocyclic ring in BT has a minimal effect on the orbitals relevant to insertion and would not be expected, per se, to favor C(aryl)−S insertion. However, the effect of η^6-precoordination on the calculated charges on C(aryl) compared to C(vinyl) prompted the suggestion that the C−M bond resulting from insertion would be stronger for C(aryl). In other words, unless sterically prohibited, η^6-precoordination favors C(aryl)−S scission. We have published[6a,b,e] high-quality X-ray crystal structures of three insertion products, **26**−**28**, and this allows an assessment of the relative bond strength of C(aryl)−Mn versus C(vinyl)−Mn in η^6-coordinated systems. As shown in Figure 9, both **26** and **27** have a C(aryl)−Mn bond length of 2.09 Å, while the C(vinyl)−Mn bond in **28** is significantly shorter at 2.04 Å. Considering these experimental results, the prediction of regioselective C(aryl)−S insertion in η^6-coordinated systems as being due to a stronger resulting C(aryl)−M bond is of questionable validity.

DFT calculations of the C(aryl)−S insertion product **26** and the C(vinyl)−S analogue **29** support the conclusions gleaned from the X-ray data. As Figure 9 shows, the Mn−C bond length is calculated to be about 0.08 Å longer in **26**, in approximate agreement with the X-ray results. The calculations also predict that the aryl insertion product **26** is more stable than the vinyl product **29** by 21 kJ/mol,[16] which agrees with the experimentally observed aryl insertion and lack of subsequent isomerization (eq 3) with benzothiophene complexes lacking a substituent at the C-7 position.

Isomerization of C(aryl)−S to C(vinyl)−S Insertion Products. A number of experiments were performed to probe the mechanism of the isomerization reaction shown in eq 3. It was previously reported[6d] that this remarkable transformation proceeds cleanly in solution at room temperature for **6** having R = Me or Et as the substituent in the 7-position. On the basis of

(15) Choi, M.-G.; Angelici, R. J. *Organometallics* **1991**, *10*, 2436. (b) Benson, J. W.; Angelici, R. J. *Organometallics* **1992**, *11*, 922. (c) Draganjac, M.; Ruffing, C. J.; Rauchfuss, T. B. *Organometallics* **1985**, *4*, 1909. (d) Goodrich, J. D.; Nickias, P. N.; Selegue J. P. *Inorg. Chem.* **1987**, *26*, 3424. (e) Rao, K. M.; Day, C. L.; Jacobson, R. A.; Angelici, R. J. *Inorg. Chem.* **1991**, *30*, 5046.

(16) Relative to **26**, **29** and **25** were found to be less stable by 21 and 160 kJ/mol, respectively. The total energies were not optimized with vibrational calculations.

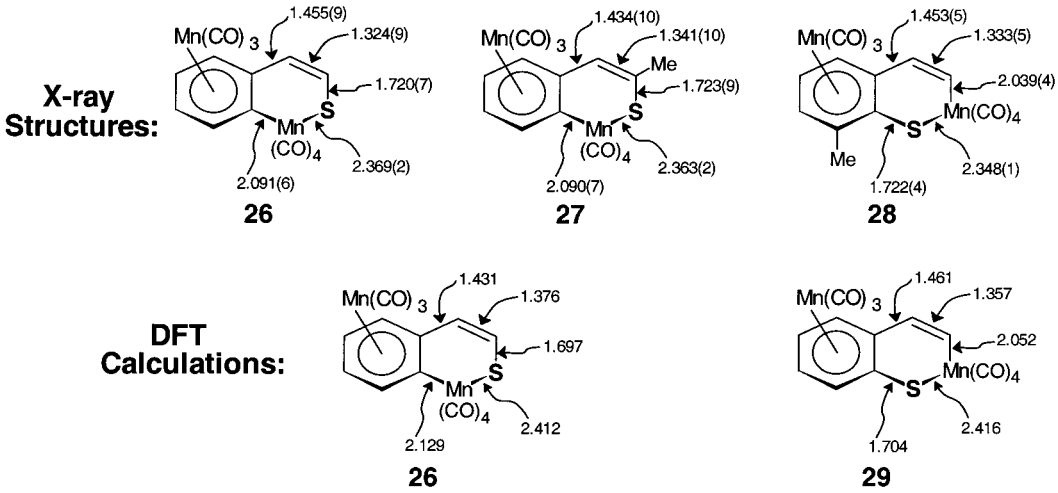

Figure 9. Comparison of bond lengths of aryl and vinyl insertion product as determined by X-ray diffraction and by DFT calculations.

Scheme 2

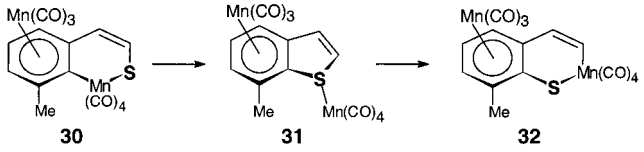

results described below, we propose the mechanism shown in Scheme 2, which involves reductive elimination from **30** to give an η^1-S intermediate **31** that reinserts into the C(vinyl)−S bond to afford the product **32**. The theoretical calculations described above indicate that **31** is a viable intermediate. Experimental evidence supporting this mechanism includes the observation that CO up to 300 psi was found to have no effect on the reaction rate ($t_{1/2}$ = 6 h at 25 °C in CH_2Cl_2). It was also found that complex **33**, in which a CO ligand is

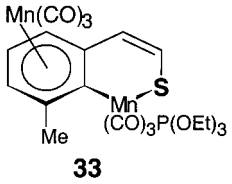

replaced with $P(OEt)_3$, does not undergo any detectable isomerization over 24 h, despite a more congested environment. It seems reasonable that the increased electron-donating properties of $P(OEt)_3$ compared to CO renders reductive elimination from **33** more difficult than from **30**. The structure of **33**, in which the phosphite ligand is in an "axial" position with respect to the heterocyclic ring, was verified by X-ray crystallography, although disorder problems prevented refinement to a publishable *R* value.

Two other experiments were done that lend support to the isomerization mechanism shown in Scheme 2. It was found that treatment of **30** with the mild oxidant ferrocenium hexafluorophosphate led to rapid deinsertion (reductive elimination) of $Mn(CO)_4$ and regeneration of the cationic benzothiophene complex **6**. Finally, as may be expected, methylation of the sulfur atom in **30**, known[6d] to be facile, was observed to block the isomerization reaction.

Conclusions

The product distribution and regiochemistry of reductive metal insertion into a C−S bond in (η^6-benzothiophene)$Mn(CO)_3^+$ complexes are greatly affected by the presence of methyl substituents at the benzothiophene 2-, 3-, and/or 7-positions. Low-temperature IR and electrochemical experiments showed that reduction at −90 °C produces (η^4-benzothiophene)$Mn(CO)_3^-$ anions, which do not react with the η^6-cation to give insertion product. Taken together, the evidence suggests a radical mechanism for the insertion of the $Mn(CO)_4$ moiety into a C−S bond. The question of which bond, C(aryl)−S or C(vinyl)−S, is activated by η^6-precoordination of the $Mn(CO)_3^+$ unit was probed by examining published crystal structures and performing DFT calculations. The conclusion, supported by both experiment and theory, is that cleavage of the C(aryl)−S bond is favored. A redetermination of the crystal structure of the η^1-S complex (η^1-3-MeBT)Re(Cp*)$(CO)_2$ revealed that the C(aryl)−S and C(vinyl)−S bonds are of similar lengths, suggesting that an η^1-S intermediate is not predisposed to insert into the latter bond, as was previously thought. DFT calculations of (η^6-BT)Mn-$(CO)_3^+$ bonded in an η^1-S fashion to $Mn(CO)_4^-$ indicated that an intermediate of this sort is viable for insertion and for C(aryl)−Mn−S to C(vinyl)−Mn−S isomerization reactions.

Experimental Section

General Procedures. Standard materials were purchased from commercial sources and used without further purification. Solvents were HPLC grade and opened under nitrogen. Literature methods were used to synthesize (η^6-benzothiophene)-$Mn(CO)_3^+$ and (η^1-3-MeBT)Re(Cp*)$(CO)_2$ (**24**) complexes.[5a,13] Low-temperature IR experiments were performed using a Remspec IR Fiber Optic Immersion Probe. Electrochemical experiments were performed with EG&G Model 173, 175, and 179 equipment.

Reductive Insertion into Complex 8. Cobaltocene (198 mg, 1.05 mmol) and [(η^6-2,3-Me_2BT)$Mn(CO)_3$]BF_4 (**8**, 388 mg, 1.0 mmol) were stirred in CH_2Cl_2 (30 mL) under an atmosphere of CO for 20 min. The reaction mixture was then eluted through a short alumina column with CH_2Cl_2. The resulting red solution was concentrated and chromatographed on a silica gel column with hexanes and then diethyl ether to afford **9**.

Yield: 60%. IR (CH_2Cl_2): ν_{CO} 2070(m), 2047(s), 1989(vs, br), 1929(m) cm^{-1}. ^1H NMR (CD_2Cl_2): δ 7.73 (d, $J = 7.6$, H7), 7.59 (d, $J = 7.7$, H4), 6.18 (t, $J = 6.9$, H6), 6.03 (td, $J = 7.4$, H5), 2.48 (s, Me), 2.30 (s, Me). Anal. Calcd for $C_{17}H_{10}SMn_2O_7$: C, 43.61; H, 2.15. Found: C, 43.52; H, 1.88. When the above procedure was repeated in the presence of 1.0 mmol of $Mn_2(CO)_{10}$ and worked up similarly, complex **10** was obtained. Yield: 69%. IR (CH_2Cl_2): ν_{CO} 2087(w), 2060(m), 2051(m), 2010(s), 1991(s), 1952(s), 1924(w), 1901(w) cm^{-1}. ^1H NMR (CD_2Cl_2): δ 6.63 (dd, $J = 6.2$, 1.5, H7), 6.32 (dd, $J = 6.4$, 1.5, H6), 6.25 (dd, $J = 6.6$, 1.5, H5), 6.19 (dd, $J = 6.6$, 1.5, H4), 2.16 (d, $J = 1.1$, Me), 2.02 (q, $J = 1.1$, Me). Dark red crystals of **10** were grown by vapor diffusion of pentane into a CH_2Cl_2 solution at −15 °C. On one occasion, a diethyl ether solution of **10** after several days at −15 °C deposited a crystal of **11**, the structure of which was determined by X-ray diffraction.

Reductive Insertion into Complex 12. Cobaltocene (190 mg, 1.0 mmol) and [(η^6-2,7-Me_2BT)$Mn(CO)_3$]BF_4 (**12**, 390 mg, 1.0 mmol) were stirred in CH_2Cl_2 (30 mL) under an atmosphere of CO for 20 min. The reaction mixture was then eluted through a short alumina column with CH_2Cl_2. The resulting red solution was concentrated and chromatographed on a silica gel column with hexanes to give **15**. Subsequent elution with diethyl ether gave two additional bands due to **13** and **14**. For **13**: yield 13%. IR (CH_2Cl_2): ν_{CO} 2065(m), 2046(s), 1977(s, br), 1928(m) cm^{-1}. ^1H NMR (CD_2Cl_2): δ 6.20 (s, H3), 6.00 (t, $J = 5.7$, H5), 5.48−5.52 (m, $J = 6.0$, H4,6), 2.76 (s, Me), 2.26 (s, Me). Anal. Calcd for $C_{17}H_{10}SMn_2O_7$: C, 43.61; H, 2.15. Found: C, 43.59; H, 1.79. For **14**: yield 10%. IR (CH_2Cl_2): ν_{CO} 2070(m), 2046(s), 1990(s, br), 1927(m) cm^{-1}. ^1H NMR (CD_2Cl_2): δ 6.68 (d, $J = 6.3$, H4), 6.29 (s, H3), 5.88 (d, $J = 6.7$, H6), 5.43 (t, $J = 6.3$, H5), 2.33 (s, Me), 2.29 (s, Me). Anal. Calcd for $C_{17}H_{10}SMn_2O_7$: C, 43.61; H, 2.15. Found: C, 43.65; H, 1.96. For **15**: yield 11%. IR (CH_2Cl_2): ν_{CO} 2074(m), 2031(s), 1974(s, br), 1950(m) cm^{-1}. ^1H NMR (CD_2Cl_2): δ 6.95 (d, $J = 5$, H4,6), 6.81 (t, $J = 4.5$, H5), 5.99 (s, H3), 2.70 (s, Me), 2.25 (s, Me). Anal. Calcd for $C_{17}H_{10}SMn_2O_7$: C, 43.61; H, 2.15. Found: C, 43.37; H, 2.60.

Reductive Insertion into Complex 16. Cobaltocene (50 mg, 0.26 mmol) and [(η^6-3,7-Me_2BT)$Mn(CO)_3$]BF_4 (**16**, 98 mg, 0.25 mmol) were stirred in CH_2Cl_2 (8 mL) under an atmosphere of CO for 25 min. The reaction mixture was concentrated and placed on a hexanes-packed alumina column. The product was eluted with CH_2Cl_2 and dried in vacuo. For **17**: yield 55%. IR (CH_2Cl_2): ν_{CO} 2065(m), 2018(s), 1971(s), 1933(m), 1917(m) cm^{-1}. ^1H NMR (CD_3COCD_3): δ 6.85 (d, $J = 5.1$, H4), 6.51 (d, $J = 6.2$, H6), 6.24 (dd, $J = 7.0$, 6.2, H5), 5.17 (d, $J = 5.1$, H2), 2.58 (s, Me), 2.35 (s, Me), −11.86 (d, $J = 5.1$, H2′). ^1H NMR (CD_2Cl_2): δ 6.29 (d, $J = 5.7$, H4), 5.80 (d, $J = 5.8$, H6), 5.60 (dd, $J = 6.5$, H5), 5.23 (d, $J = 5.3$, H2), 2.52 (s, Me), 2.28 (s, Me), −11.51 (d, $J = 5.1$, H2′). HR MS for M+ calcd 300.9732; found 300.9747. Anal. Calcd for $C_{17}H_{10}SMn_2O_7$: C, 39.33; H, 1.91. Found: C, 39.87; H, 1.97.

Synthesis of Insertion Complex 33. To cobaltocene (109 mg, 0.58 mmol) and $P(OEt)_3$ (1 mmol) in CH_2Cl_2 (10 mL) was added [(η^6-7-MeBT)$Mn(CO)_3$]BF_4 (145 mg, 0.39 mmol), and the reaction mixture was stirred under N_2 for 30 min. The deep red solution was concentrated and chromatographed on neutral alumina wetted with hexanes, and eluted with diethyl ether. Further purification was achieved by TLC on silica gel with a 1:1 solution of Et_2O/hexanes. Yield: 74%. IR (CH_2Cl_2): ν_{CO} 2050(s), 2003(s), 1990(m), 1931(m), 1890(m) cm^{-1}. ^1H NMR (CD_3COCD_3): δ 7.32 (d, $J = 9.5$, H2), 6.36 (d, $J = 6.6$, H4), 6.21 (d, $J = 9.5$, H3), 5.95 (m, H5), 5.76 (d, $J = 6.8$, H6), 2.52 (s, Me), 3.95 (m, 6H, OCH_2), 1.16 (m, 9H, OCH_2CH_3).

Density Functional Theory Calculations. All input structures for complexes **25**, **26**, and **29** were generated with the PCMODEL molecular modeling program and minimized with the MMX force field.[17] The structures were completely optimized in redundant internal coordinates through density functional theory calculations (DFT) as implemented in the NWChem 4.0 package of programs.[18] NWChem was run on a 3-node RedHat Linux cluster. Each node was a Penguin Computing Neveus workstation with dual 850 MHz Pentium III processors (six processors in total) with a collective 1.5 GB of RAM. The DFT optimizations used Becke's three-parameter functional (B3) along with the Lee−Yang−Parr correlation functional (LYP).[19] All DFT optimizations employed the double-ζ-split-valence + polarization (DZVP) basis set.[20] Each calculation required approximately 30 days for completion.

Acknowledgment. This work was supported in part by grant CHE-9705121 from the National Science Foundation. Acknowledgment is made to donors of the Petroleum Research Fund, administered by the ACS, for partial support of this research. We also acknowledge financial support from the Committee to Aid Faculty Research of Providence College. We are grateful to Professor Robert J. Angelici for helpful discussions and for providing structure factor data for complex **24** that was used in ref 13.

Supporting Information Available: Tables of atomic coordinates, bond lengths and angles, anisotropic displacement parameters, hydrogen coordinates, and torsion angles for **10**, **11**, **15**, **17**, and **24**. This material is available free of charge via the Internet at http://pubs.acs.org.

OM0108907

(17) *MMX* force field (1999); Serena Software: P.O. Box 3076, Bloomington, IN 47402.

(18) Harrison, R. J.; Nichols, J. A.; Straatsma, T. P.; Dupuis, M.; Bylaska, E. J.; Fann, G. I.; Windus, T. L.; Apra, E.; Anchell, J.; Bernholdt, D.; Borowski, P.; Clark, T.; Clerc, D.; Dachsel, H.; de Jong, B.; Deegan, M.; Dyall, K.; Elwood, D.; Fruchtl, H.; Glendenning, E.; Gutowski, M.; Hess, A.; Jaffe, J.; Johnson, B.; Ju, J.; Kendall, R.; Kobayashi, R.; Kutteh, R.; Lin, Z.; Littlefield, R.; Long, X.; Meng, B.; Nieplocha, J.; Niu, S.; Rosing, M.; Sandrone, G.; Stave, M.; Taylor, H.; Thomas, G.; van Lenthe, J.; Wolinski, K.; Wong, A.; Zhang, Z. *NWChem, A Computational Chemistry Package for Parallel Computers, Version 4.0*; Pacific Northwest National Laboratory: Richland, WA 99352, 2000.

(19) Becke, A. D. *J. Chem. Phys.* **1993**, *98*, 5648. (b) Lee, C.; Yang, W.; Parr, R. G. *Phys. Rev. B* **1988**, *37*, 785.

(20) Godbout, N.; Salahub, D. R.; Andzelm, J.; Wimmer, E. *Can. J. Chem.* **1992**, *70*, 560.